

## RESEARCH ARTICLE

# Data augmentation for design of concentric tube continuum robots by generative adversarial networks

Matthias K. Hoffmann<sup>1</sup> | Rutwik Gulakala<sup>2</sup> | Julian Mühlenhoff<sup>3</sup>  |  
Zhaoheng Ding<sup>3</sup> | Thomas Sattel<sup>3</sup> | Marcus Stoffel<sup>2</sup> | Kathrin Flaßkamp<sup>1</sup>

<sup>1</sup>Systems Modeling and Simulation,  
Saarland University, Saarbrücken,  
Germany

<sup>2</sup>Institute of General Mechanics, RWTH  
Aachen University, Aachen, Germany

<sup>3</sup>Mechatronics Group, Technische  
Universität Ilmenau, Ilmenau, Germany

## Correspondence

Julian Mühlenhoff, Technische  
Universität Ilmenau, Ilmenau, 98693,  
Germany.

Email:

[julian.muehlenhoff@tu-ilmenau.de](mailto:julian.muehlenhoff@tu-ilmenau.de)

## Funding information

German Research Foundation,  
Grant/Award Numbers: 501928699,  
501877598, 461953135

## Abstract

Concentric tube continuum robots are a promising type of robot for various medical applications. Their application in neurosurgery poses challenging requirements for design and control that can be addressed by physics-informed data-based approaches. A prerequisite to data-based modeling is an informative, rich data set. However, limited access to experimental data raises interest in partially or entirely synthetic data sets. In this contribution, we study the application of generative adversarial networks (GANs) for data augmentation in a data-based design process of such robots. We propose a GAN framework suitable for curve-fitting to generate synthetic trajectories of robots along with their corresponding control parameters. Our evaluation shows that the GANs can efficiently produce meaningful synthetic trajectories and control parameter pairs that show a good agreement with simulated trajectories.

## 1 | INTRODUCTION

Continuum robots are a class of robots without any presence of joints, whose movement is achieved by continuous deformation of the robot's backbone. There are different types of continuum robots; however, concentric tube continuum robots (CTCRs) are seen as a well-suited robotic principle for accessing targets hidden by obstacles on a slender pathway [1]. For this, CTCRs combine a set of precurved and hollow tubes with ascending diameters nested into each other. By rotational as well as translational actuation at each tube's base, the robot's backbone pose is established throughout the tubes' elastostatic bending interaction, as can be seen in Figure 1.

In particular, CTCRs have been proposed as steerable surgical needles to access deep-sited medical targets with minimum damage to surrounding tissue through keyhole body openings [1–3]. For achieving high target precision, the combined planning problem of design and actuation has to be carried out, that is, determining geometrical parameters of the tubes as well as actuation parameters for translation and rotation by avoiding given obstacles [4, 5]. Therefore, the planning's overall accuracy heavily relies on the accuracy of the used physical model. While several publications focus on increasing model coverage [6, 7], the downside is a further increased modeling effort with many phenomenological parameters to be measured or identified and a potential to overfit these models. Hence, learning-based approaches for modeling CTCRs are seen as promising [8].

This is an open access article under the terms of the [Creative Commons Attribution-NonCommercial-NoDerivs](https://creativecommons.org/licenses/by-nc-nd/4.0/) License, which permits use and distribution in any medium, provided the original work is properly cited, the use is non-commercial and no modifications or adaptations are made.

© 2023 The Authors. *Proceedings in Applied Mathematics & Mechanics* published by Wiley-VCH GmbH.

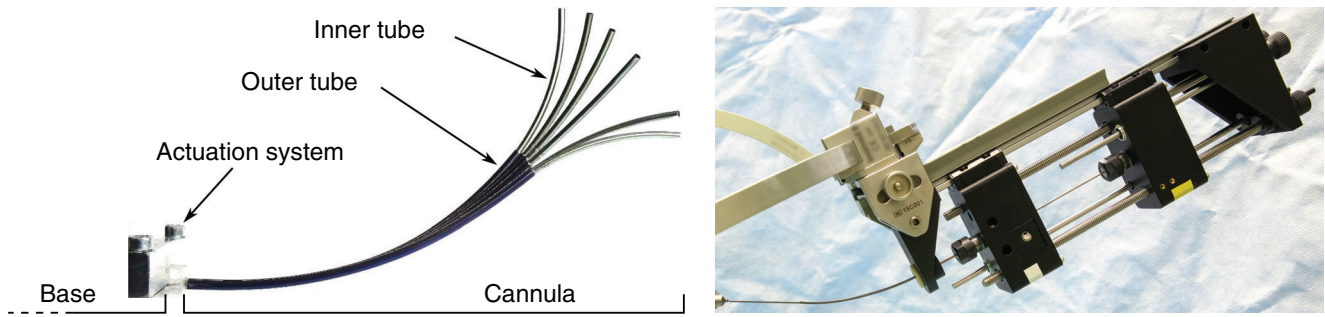


**FIGURE 1** Left: movement principle of a two-tube CTCR with the inner tube performing a rotation by  $180^\circ$ . Right: exemplary manually controlled, two-tube actuation system for stereotactic neurosurgery research.

To learn the relation between CTCR parameters and the resulting backbone shape, a densely sampled and valid data set of accurate measurements is needed. However, manufacturing of hundreds of CTCR variants for a densely sampled parameter space is too time-consuming. Therefore, this paper aims at augmenting loosely sampled CTCR data with the application of generative adversarial networks (GANs), to fill the missing gaps in the experimental data.

## 1.1 | Concentric tube continuum robots

The CTCR backbone shape follows from forces acting between the concentrically arranged tubes and the elastostatic reaction to them toward an equilibrium state. These forces mainly arise from bending as well as torsion, because shear and tension can be neglected for slender mechanical rods as a good approximation [9]. The combined torsional and bending problem already exposes ambiguity regarding the results, that is, that one set of actuation variables can lead to different backbone shapes with respect to actuation history [10]. Such models are computationally efficient and are seen as a modeling baseline [2], but exhibit position errors of up to 10% of their actuated length in high-torsion or high-bending configurations, which is considered too high for neurosurgical plannings [3].

Actuation system cyclic tests indicate that tube clearances, as well as friction forces, have a significant influence on the resulting backbone shape [3, 6, 7]. Furthermore, nickel–titanium, the material oftentimes used for the tubes, exhibits nonlinear and hysteretic stress–strain behavior [7]. Such effects have been implemented into separate physically motivated CTCR models; however, an integration of all of these effects into one simulation model would be challenging due to complexity, parameter identification, and computation effort, especially for usage in path planning.

Instead of using highly phenomenological models with large amounts of parameters to be identified, another approach is to apply machine learning methods directly as a simulation or control technique. For the simulation problem, several works estimate the tip's pose or the entire CTCR shape in dependency of the actuation parameters [11–13]. The problem of path planning or control is addressed by the inverse relation with similar methods [12, 14–16]. Such approaches rely on a densely sampled and valid data set of high measurement accuracy, which is time-consuming to establish [17]. For that reason, some authors stick with learning other physical models [14–16]. Kuntz et al. are using a combination of measurements and simulation data [13]. Measurements are typically carried out by photogrammetry [3, 7, 9], electromagnetic tracking systems [11, 17], or fiber optical systems [18], whereas only photogrammetry is able to measure the backbone instead of just the tip.

## 1.2 | Data augmentation methods

Neural networks have shown great results throughout a large variety of fields including image classification [19, 20], natural language processing [21], and data-driven modeling [22, 23]. However, these networks often suffer the problem of overfitting, an effect where the network memorizes the training data without generalizing well for inputs that were not part of the training data. This effect can be detected via a split of the data into training, validation, and test data, each containing exclusively differing data.

While there are many approaches to reduce overfitting (early-stopping, regularization, dropout, etc.), the problem arises from the insufficient variance of the training data and the high number of parameters these models feature. Thus, data augmentation methods are employed to synthetically enlarge the data sets by introducing variations of the known data. For images, for example, translation and rotation of objects can be introduced as the transformed object is typically still from the same category.

In addition to these geometrical variations, generative models like GANs, variational autoencoders (VAEs), or denoising diffusion probabilistic models (DDPMs) can be used to generate artificial data, similar but different to the data from the original data set while maintaining crucial features. The survey by Shorten et al. [24] gives a thorough summary of data augmentation methods for images, which can be more or less directly applied to our use case.

### 1.3 | Contributions and outline

This work demonstrates the applicability of GANs for augmenting positional backbone data of CTCRs to enrich these data sets. In the following Section 2, generative adversarial models are introduced. Section 3 describes the data generation process and the physical model used for generating the training data. Section 4 presents the results of using GANs for generating artificial cannula data. Section 5 summarizes the work and gives an overview over future work.

## 2 | GENERATIVE ADVERSARIAL NETWORKS

GANs are an approach to generative modeling using deep learning methods. They are a class of algorithms that can generate artificial data from sampled latent vectors, dimensional latent space, or from a given condition set. They possess the ability to generate a new multidimensional tensor space that can aptly represent the underlying data distribution of the problem domain forming a compressed representation of the data distribution. The GAN framework typically consists of two deep networks, namely, a generator and a discriminator. These two neural networks compete with each other in a min-max game or a zero-sum game, where one network's gain is the other network's loss. The loss function of the GAN is expressed by

$$\min_G \max_D V(G, D) = E_x[\log(D(x))] + E_z[\log(1 - D(G(z)))]. \quad (1)$$

Here,  $G$  represents the generator,  $D$  represents the discriminator,  $D(x)$  represents the output of real input,  $E_x$  is the target or actual output over all the real data instances, and  $G(z)$  is the output generated by the generator with given noise  $z$ . The output of the discriminator for a generated input for a sample  $z$  is denoted by  $D(G(z))$  and  $E_z$  is the expected value over all random inputs to the generator. Usually, the networks are designed with one discriminator and one generator but there are frameworks with multiple discriminators and generators per framework proposed in the literature. A lot of generator and discriminator architectures have been developed since their inception. GANs have been widely used in large language models [25, 26], image segmentation, deep fakes and upscaling [27–29], and disease diagnosis [19, 20].

In this study, we use a multilayer perceptron-based generator and discriminator architecture. The general framework of the proposed architecture is shown in Figure 2. Due to the nature of the losses and the adversarial process, it is difficult to assess the training of the GAN and this makes them notoriously hard to train, even for classification tasks. Given that we employ the framework for curve fitting, it exponentially increases this difficulty. Hence, to reduce the training effort, we implement an autoencoder network to shrink the dimensionality of the data to a latent space of dimensionality 6, making it comparatively easier for the GAN to train.

## 3 | DATA GENERATION

It is hard to predict the amount of data, and, correspondingly, its diversity, which is necessary for training a neural network. To estimate the required amount of measurements with real cannula configurations, we perform a simulation-based study here. Simulation data allow to sample the parameter space arbitrarily fine, and thus, to estimate lower limits for the amount of data. Another advantage of this methodology is the possibility of comparing generative adversarial network

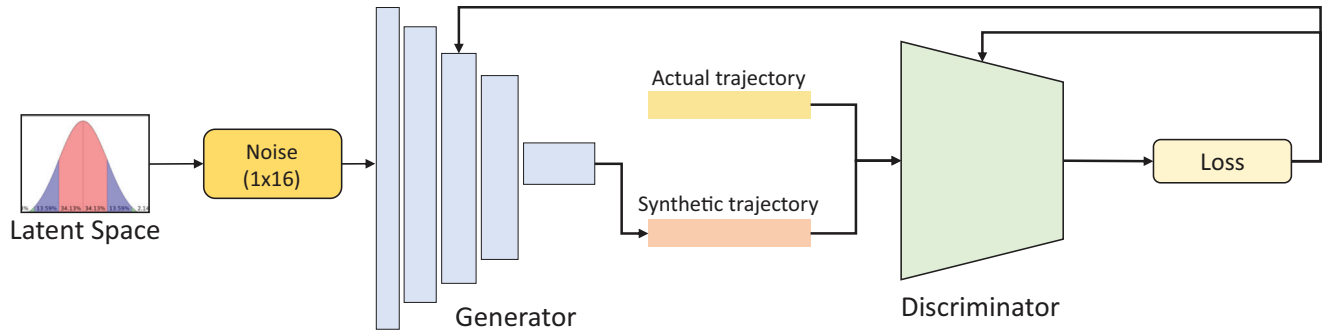


**FIGURE 2** Framework of the GAN in this work.

(GAN) results with the corresponding simulation, which is not possible if arbitrary tube configurations are generated by the GAN. We also restrict our problem to two-tube CTCRs as a starting point. Eventually, our goal is to use the models trained in this scope on low-fidelity simulation data and refine them using real-world data.

### 3.1 | Simulation model

To obtain the simulation data, we implemented the CTCR model from Rucker [9]. This model describes the tubes' backbones as Frenet–Serret formulas and assumes an elastostatic equilibrium due to bending and torsion between these tubes, which leads to a boundary value problem (BVP) for the torsional angles. While there are more accurate CTCR models available, it can be seen as a good starting point for the scope of this paper with respect to calculation time.

For the implementation, we have chosen an object-oriented approach inside the Python programming language to keep track of the different variables and methods for each tube and the CTCR, respectively. The central BVP is solved via a shooting approach.<sup>1</sup> Other solvers or methods have found to be less stable or less efficient.<sup>2</sup> After solving the boundary value problem, the final CTCR backbone shape is determined by integration of the Frenet–Serret formulas using an explicit Runge–Kutta method<sup>3</sup> with reinitializations at every tube's ending accounting for discontinuities.

The resulting simulation result is heavily relying on the initial guess for the torsional component inside the BVP due to the ambiguity of the CTCR itself [10] when it comes to torsion. Depending on the initial guesses, either no result at all or multiple results can be found. The torsional ambiguity also depends on the kinematic history of the CTCR, because small actuations usually result in small backbone changes, as long as no snapping occurs. Taking this into account, for the two-tube CTCRs considered here, we apply a relative rotation between the tubes with gradually incrementing relative angle  $\Delta\alpha = 0, \dots, \pm\pi$ , while taking the last solution as initial guess for the next solution. After that, common rotations of both tubes  $\alpha_1$  and  $\alpha_2$  can be calculated by just performing this rotation on the backbone shape result, because only the actuation angle difference  $\Delta\alpha$  leads to different results for the BVP.

### 3.2 | Screening of control input and design space

In this work, we focus on generating data for one cannula configuration shown in Table 1. The rotations  $\alpha_i$  and translations  $\beta_i$  are sampled in 16 steps between  $[-\pi, \pi)$  and  $[-L_i, 0]$ , respectively. To save simulation time, CTCR simulations were performed on an AMD Ryzen Threadripper PRO 5965WX CPU with 48 parallel worker processes, which, on average, takes 1 s of calculation time per variant. Since the solutions corresponding to  $(\alpha_1, \alpha_2)$  and  $(-\alpha_1, -\alpha_2)$  are mirror symmetric in three-dimensional space, we can obtain the solutions corresponding to  $\alpha_2 \in [-\pi, 0]$  by transforming the existing solutions. For training, 40 000 of these 65 536 data points were randomly selected and split between 40% training, 40% validation, and 20% test data.

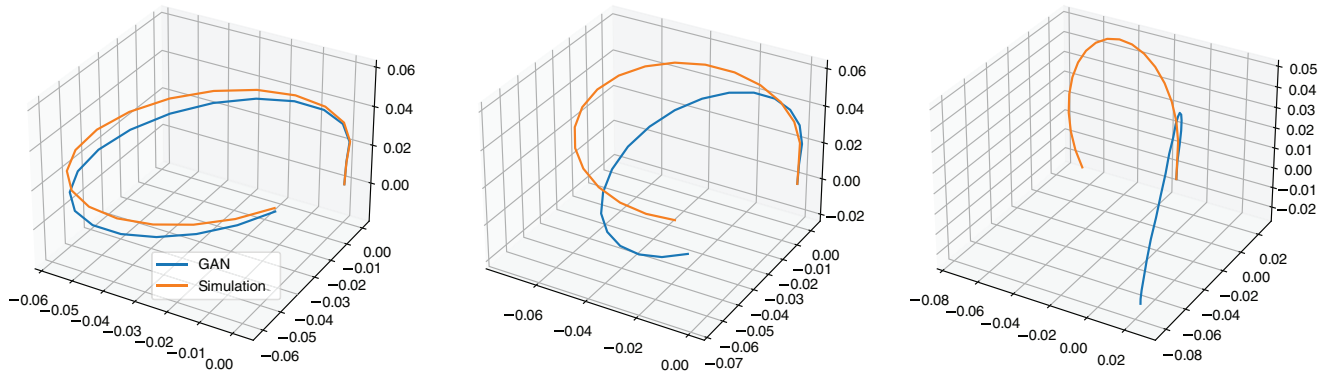
<sup>1</sup> `scipy.optimize.root()` with solver `hybr` as outer root search.

<sup>2</sup> We tested applicable solvers from `scipy.optimize.root()` as well as `scipy.integrate.solve_bvp()`.

<sup>3</sup> `scipy.integrate.solve_ivp()` with solver `RK45`.

**TABLE 1** Cannula configuration with tube parameters used for data generation.

|        | $d_o$ in mm<br>Outer diameter | $d_i$ in mm<br>Inner diameter | $L$ in mm<br>Tube length | $E$ in GPa<br>Young's modulus | $\nu$<br>Poisson's ratio | $u^*$ in 1/m<br>Precurvature |
|--------|-------------------------------|-------------------------------|--------------------------|-------------------------------|--------------------------|------------------------------|
| Tube 1 | 1.524                         | 1.296                         | 336                      | 58                            | 0.3448                   | [0, 25, 0]                   |
| Tube 2 | 2.32                          | 1.88                          | 142                      | 58                            | 0.3448                   | [0, 11.11, 0]                |

**FIGURE 3** Plots depicting the synthetic trajectory obtained from GANs versus simulated trajectory for the corresponding control parameters obtained for the GAN.

## 4 | NUMERICAL PROCEDURE AND EVALUATION

### 4.1 | Details on hyperparameters for learning

The simulations and neural network training were done in Python. The autoencoder was trained using Pytorch and the GAN training was realized in Tensorflow. The autoencoder's encoder and decoder consist of five hidden layers with 50 neurons and ELU (exponential linear unit) activation. The generator of the GAN is based on a densely connected network with six hidden layers and 100 neurons in total and a combination of Leaky ReLU, SeLU, and Tanh activation functions. The discriminator is also a densely connected network with five hidden layers and 76 neurons in total with Leaky ReLU in all the layers and sigmoid in the final layer. The aim of the discriminator is to get an estimated likelihood of the similarity of the generated data to the actual distribution. A learning rate of  $4 \times 10^{-4}$  for the generator and  $10^{-3}$  for the discriminator are chosen and Adam optimizer for calculating and applying the gradients. The generator is trained on a weighted combination of cross entropy and L1-norm regularization losses with weighted coefficients, where the cross entropy is weighted by a factor of 0.3 and the L1-norm by a factor of 0.7.

### 4.2 | Results

The GAN is trained for 800k epochs and 256 synthetic datapoints have been generated from the generator for evaluation. The synthetic trajectories are compared with simulated trajectories, computed using the control parameters the GAN generated along the points along the backbone. Figure 3 shows three synthetic data with their corresponding reconstruction.

We find that the generated CTCRs show a smooth curve backbone and that the shape is very close to the shape of the simulated tube, but the rotation seems to be faulty in many cases. Even though these results are not directly usable as is, they give hope that the results become better if the loss is changed to give more weight to the rotation angle in the autoencoder. Generating 256 datapoints using the GAN takes 15.6 ms and decoding these another 15.8 ms, resulting in an average time per sample of 0.12 ms, a major speedup compared to 1 s per simulation.

### 4.3 | Discussion from methodological viewpoint

The proposed GAN framework has been able to generate synthetic trajectories that agree with realistic simulation results if the errors, probably stemming from the autoencoder, are neglected. Still, the GAN shows to perform satisfactorily for the given task. The loss plays an important role in training the networks and it is crucial that a suitable loss is developed for the autoencoder and the GANs to perform better. Unlike other architectures, where mean squared error is highly desired for curve-fitting, GANs, however, cannot be trained just with the said loss.

## 5 | CONCLUSION AND FUTURE WORK

In this work, we evaluate data augmentation based on GANs for generating positions along a discretized backbone of a CTCR. We show that GANs have the potential to generate physically meaningful data, but that—similar to the generation of image data—the training is difficult and needs fine-tuning, such that in our work, the predicted angle is off. Still, the high quality of the overall backbone shape confirms that GANs should be investigated to enrich data sets for CTCRs. The generation process for 256 samples takes 31.4 ms, so it was found to be much faster than simulations that took an average 1 s, emphasizing that GANs allow for fast generation of synthetic cannula data. The performance of the GAN can be improved further with customized loss functions suitable for curve-fitting for both generator and discriminator networks.

In the future, we will compare GANs with other generative model types such as DDPMs and VAEs for applicability in CTCR design, as these models differ in data quality, training effort, and inference time. With an extensive data set, these comparisons should be made using real cannula data from a photogrammetric system, while including more variability than just the control parameters to additionally contain data for different tube parameters.

### ACKNOWLEDGMENTS

The authors were financially supported by German Research Foundation (DFG) Priority Programme SPP 2353 (project numbers 501928699 and 501877598) as well as by DFG project number 461953135.

Fabian Rabel has contributed to the mechanical design of the CTCR actuation system, depicted in Figure 1 on the right, as a scientific employee at Mechatronics Group, Technische Universität Ilmenau.

Open access funding enabled and organized by Projekt DEAL.

### ORCID

Julian Mühlenhoff  <https://orcid.org/0009-0003-0256-6171>

### REFERENCES

- da Veiga, T., Chandler, J. H., Lloyd, P., Pittiglio, G., Wilkinson, N. J., Hoshiar, A. K., Harris, R. A., & Valdastrì, P. (2020). Challenges of continuum robots in clinical context: A review. *Progress in Biomedical Engineering*, 2(3), 032003.
- Burgner-Kahrs, J., Rucker, D., & Choset, H. (2015). Continuum robots for medical applications: A survey. *IEEE Transactions on Robotics*, 31(6), 1261–1280.
- Mühlenhoff, J., Körbner, T., Miccoli, G., Keiner, D., Hoffmann, M. K., Sauerteig, P., Worthmann, K., Flasskamp, K., Urbschat, S., Oertel, J., & Sattel, T. (2022). A manually actuated continuum robot research platform for deployable shape-memory curved cannulae in stereotactic neurosurgery. In *International Conference and Exhibition on New Actuator Systems and Applications* (pp. 1–4). VDE Verlag.
- Flaßkamp, K., Worthmann, K., Mühlenhoff, J., Greiner-Petter, C., Büskens, C., Oertel, J., Keiner, D., & Sattel, T. (2020). Towards optimal control of concentric tube robots in stereotactic neurosurgery. *Mathematical and Computer Modelling of Dynamical Systems*, 25(6), 560–574.
- Sauerteig, P., Hoffmann, M. K., Mühlenhoff, J., Miccoli, G., Keiner, D., Urbschat, S., Oertel, J., Sattel, T., Flaßkamp, K., & Worthmann, K. (2022). Optimal path planning for stereotactic neurosurgery based on an elastostatic cannula model. *IFAC-PapersOnLine*, 55(20), 600–605. 10th Vienna International Conference on Mathematical Modelling 2022.
- Ha, J., Fagogenis, G., & Dupont, P. (2019). Modeling tube clearance and bounding the effect of friction in concentric tube robot kinematics. *IEEE Transactions on Robotics*, 35(2), 353–370.
- Greiner-Petter, C., & Sattel, T. (2017). On the influence of pseudoelastic material behavior in planar shape-memory tubular continuum structures. *Smart Materials and Structures*, 26(12).
- Wang, X., Li, Y., & Kwok, K. W. (2021). A survey for machine learning-based control of continuum robots. *Frontiers in Robotics and AI*, 8, 1–14.
- Rucker, D. C., Jones, B. A., & Webster III, R. J. (2010). A geometrically exact model for externally loaded concentric-tube continuum robots. *IEEE Transactions on Robotics*, 26(5), 769–780.

10. Rucker, D. C., Webster III, R. J., Chirikjian, G. S., & Cowan, N. J. (2010). Equilibrium conformations of concentric-tube continuum robots. *The International Journal of Robotics Research*, 29(10), 1263–1280.
11. Fagogenis, G., Bergeles, C., & Dupont, P. E. (2016). Adaptive nonparametric kinematic modeling of concentric tube robots. In *International Conference on Intelligent Robots and Systems* (pp. 4324–4329). IEEE.
12. Grassmann, R., Modes, V., & Burgner-Kahrs, J. (2018). Learning the forward and inverse kinematics of a 6-dof concentric tube continuum robot in se(3). In *International Conference on Intelligent Robots and Systems* (pp. 5125–5132). IEEE.
13. Kuntz, A., Sethi, A., Webster III, R. J., & Alterovitz, R. (2020). Learning the complete shape of concentric tube robots. *IEEE Transactions on Medical Robotics and Bionics*, 2(2), 140–147.
14. Iyengar, K., Dwyer, G., & Stoyanov, D. (2020). Investigating exploration for deep reinforcement learning of concentric tube robot control. *Journal of Computer Assisted Radiology and Surgery*, 15, 1157.
15. Iyengar, K., & Stoyanov, D. (2021). Deep reinforcement learning for concentric tube robot control with a goal-based curriculum. In *International Conference on Robotics and Automation* (pp. 1459–1465). IEEE.
16. Liang, N., Grassmann, R. M., Lilge, S., & Burgner-Kahrs, J. (2021). Learning-based inverse kinematics from shape as input for concentric tube continuum robots. In *International Conference on Robotics and Automation* (pp. 1387–1393). IEEE.
17. Grassmann, R. M., Chen, R. Z., Liang, N., & Burgner-Kahrs, J. (2022). A dataset and benchmark for learning the kinematics of concentric tube continuum robots. In *International Conference on Intelligent Robots and Systems* (pp. 9550–9557). IEEE.
18. Xu, R., Yurkewich, A., & Patel, R. V. (2016). Shape sensing for torsionally compliant concentric-tube robots. In *Optical Fibers and Sensors for Medical Diagnostics and Treatment Applications XVI*, SPIE.
19. Gulakala, R., Markert, B., & Stoffel, M. (2023). Rapid diagnosis of covid-19 infections by a progressively growing gan and cnn optimisation. *Computer Methods and Programs in Biomedicine*, 229(C).
20. Gulakala, R., Markert, B., & Stoffel, M. (2022). Generative adversarial network based data augmentation for cnn based detection of covid-19. *Scientific Reports*, 12(1), 19186.
21. Wolf, T., Debut, L., Sanh, V., Chaumond, J., Delangue, C., Moi, A., Cistac, P., Rault, T., Louf, R., Funtowicz, M., Davison, J., Shleifer, S., von Platen, P., Ma, C., Jernite, Y., Plu, J., Xu, C., Le Scao, T., Gugger, S., ... Rush, A. (2020). Transformers: State-of-the-art natural language processing. In *Conference on Empirical Methods in Natural Language Processing: System Demonstrations* (pp. 38–45). Association for Computational Linguistics.
22. Stoffel, M., Gulakala, R., Bamer, F., & Markert, B. (2020). Artificial neural networks in structural dynamics: A new modular radial basis function approach vs. convolutional and feedforward topologies. *Computer Methods in Applied Mechanics and Engineering*, 364, 112989.
23. Gulakala, R., Markert, B., & Stoffel, M. (2023). Graph neural network enhanced finite element modelling. *PAMM*, 22(1), e202200306.
24. Shorten, C., & Khoshgoftaar, T. M. (2019). A survey on image data augmentation for deep learning. *Journal of Big Data*, 6(1), 1–48.
25. Brown, T., Mann, B., Ryder, N., Subbiah, M., Kaplan, J. D., Dhariwal, P., Neelakantan, A., Shyam, P., Sastry, G., Askell, A., Agarwal, S., Herbert-Voss, A., Krueger, G., Henighan, T., Child, R., Ramesh, A., Ziegler, D., Wu, J., Winter, C., ... Amodei, D. (2020). Language models are few-shot learners. In *Advances in Neural Information Processing Systems* (pp. 1877–1901). Curran Associates.
26. Touvron, H., Lavril, T., Izacard, G., Martinet, X., Lachaux, M. A., Lacroix, T., Rozière, B., Goyal, N., Hambro, E., Azhar, F., Rodriguez, A., Joulin, A., Grave, E., & Lample, G. (2023). Llama: Open and efficient foundation language models.
27. Park, T., Liu, M. Y., Wang, T. C., & Zhu, J. Y. (2019). Semantic image synthesis with spatially-adaptive normalization. In *Conference on Computer Vision and Pattern Recognition* (pp. 2332–2341). IEEE.
28. Karras, T., Laine, S., & Aila, T. (2021). A style-based generator architecture for generative adversarial networks. *IEEE Transactions on Pattern Analysis and Machine Intelligence*, 43(12), 4217–4228.
29. Watson, A. (2020). Deep learning techniques for super-resolution in video games.

**How to cite this article:** Hoffmann, M. K., Gulakala, R., Mühlhoff, J., Ding, Z., Sattel, T., Stoffel, M., & Flaßkamp, K. (2023). Data augmentation for design of concentric tube continuum robots by generative adversarial networks. *Proceedings in Applied Mathematics and Mechanics*, 23, e202300278.  
<https://doi.org/10.1002/pamm.202300278>